ELSEVIER

Journal of Magnetism and Magnetic Materials 247 (2002) 270–278

journal of magnetism and magnetic materials

www.elsevier.com/locate/jmmm

Anisotropic properties of rare-earth dibismites

C. Petrovic*, S.L. Bud'ko, P.C. Canfield

Ames Laboratory and Department of Physics and Astronomy, Iowa State University, Ames, Iowa 50011, USA

Received 11 January 2002; received in revised form 13 March 2002

Abstract

We report measurements of magnetic, thermal and transport properties of single crystals of rare-earth dibismites RBi_2 (R = La–Nd, Sm), grown via self-flux method. All compounds are good metals, and those with magnetic ions order antiferromagnetically at low temperatures. Ce, Pr and Sm members of the series show single magnetic transition whereas $NdBi_2$ most likely exhibits two magnetic transitions. Significant magnetic anisotropy and a series of metamagnetic transitions in fields up to 55 kG are found in $PrBi_2$. Ordering temperatures range from 3 K to just above 16 K and they scale well with the de Gennes factor.

PACS: 75.30.G; 75.50; 75.60.E; 75.40

Keywords: Crystal growth; Heat capacity; Magnetic anisotropy; Rare-earth dibismites

1. Introduction

Motivated by interesting physical properties of rare-earth diantimonides [1–4] we have synthesized and performed detailed magnetic, thermodynamic and electrical transport measurements on another rare-earth series that crystallizes in similar quasi-2D crystal structure. The physical properties of compounds found at the Bi-rich side of R–Bi binary phase diagrams have not been studied in much detail. The compounds RBi_2 (R = La–Nd) were first synthesized in 1975 as a new structure type in polycrystalline form [5], but space group and crystal structure type have not been determined so far. A polycrystalline $LaBi_2$ sample has been indexed with an orthorhombic unit cell several years after initial discovery [6]. Lattice constants (without space group determination) were $a = 4.737$ Å, $b = 17.51$ Å, $c = 4.564$ Å.

In this paper, we present the results of detailed measurements on single crystals of RBi_2 series (R = La–Nd, Sm). Temperature and field-dependent resistivity and magnetization data, as well as temperature-dependent specific heat data reveal that the RBi_2 series is similar to the RSb_2 series in terms of magnetic properties, but in contrast to the RSb_2 series, manifest only modest magnetoresistivity. In addition, no de Haas van Alphen or Shubnikov de Haas oscillations have been observed for $T > 1.8$ K and $H < 55$ kOe.

2. Sample preparation and experimental techniques

Large single crystals of RBi_2 were grown from a binary melt with an initial composition $R_{0.08}Bi_{0.92}$.

*Corresponding author. Tel.: +1-515-294-3986; fax: +1-515-294-0689.

E-mail address: petrovic@ameslab.gov (C. Petrovic).

0304-8853/02/$ - see front matter
PII: S0304-8853(02)00278-0

The elemental constituents were placed in an alumina crucible and sealed in a quartz ampoule in vacuum. The melt was heated up to 1100°C, fast cooled to 1000°C (in the case of La and Pr) or to 850°C (for R = Ce, Nd, Sm) and then cooled to 400°C (R = La, Pr) and 500°C (other rare earths) over 120 h [7–9]. Crystals grew in the shape of malleable layered plates that can easily be exfoliated. Powder X-ray diffraction, therefore, is rather difficult, and several samples on which it was performed yielded only broad Bi peaks. Nevertheless, R–Bi binary phase diagrams, plate-like morphology and magnetic susceptibility (discussed below) indicate RBi_2 stoichiometry. Gd–Bi binary melt gave cubic crystals that showed long-range magnetic order around 25 K and Curie tail in high-temperature susceptibility consistent with GdBi stoichiometry. Eu–Bi melt also gave cubic crystals whose Curie tail (assuming Eu^{2+}) was consistent with $EuBi_3$ stoichiometry. However, no Bi-rich Eu–Bi binaries have been reported so far. Due to malleability of the samples, powder X-ray diffraction data were inconclusive. Although the existence of $GdBi_2$ compound has been proposed, our melts with 8% Gd still produced GdBi, indicating that the incongruent melting point of hypothetical $GdBi_2$ phase (if it exists at all) should be moved to temperatures lower than 500°C [10]. Heavier rare earths do not make in this stoichiometry.

Anisotropic field and temperature-dependent magnetization measurements were made using a Quantum Design MPMS-5 SQUID magnetometer in temperature range $T = (1.8-300)$ K and in magnetic fields up to 55 kOe, applied parallel to the ab plane or *c*-axis of the crystal. The polycrystalline value of magnetization was obtained, disregarding possible in-plane magnetic anisotropy, by $\chi_{poly} = \chi_c/3 + 2\chi_{ab}/3$.

In-plane resistance was measured using LR 400 and LR 700 resistance bridges with the standard four-probe method using MPMS as a H, T platform. Since all samples were cut into large rods, there was little ambiguity in the determination of the geometrical factor. Due to extremely high air sensitivity of samples, some electrical contacts have been made with silver paint rather than silver epoxy so as to avoid the need to heat the sample above 300 K. Specific heat was measured in the Quantum Design PPMS system using a relaxation technique with power-law fit of the temperature response. Magnetic ordering temperatures have been obtained by determination of the maximum in $\partial(\chi T)/\partial T, \partial\rho/\partial T$ and thermodynamic anomaly in specific heat data.

Collection of electrical transport data on this series involved difficulties associated with the rapid decomposition and oxidation of samples on air [5]. The rate of decomposition is greatly enhanced by sample heating and thermal cycling. Aging of the samples introduces some irreproducibility in magnetic susceptibility and resistivity data, making detailed measurements much more difficult than in the case of RSb_2. It is likely that this crystal structure forms with more defects towards the end of the series, since Gd and heavier dibismites could not be obtained. The trend of decreasing residual resistivity ratio (RRR) from La to Nd and Sm dibismite also speaks in favor of this hypothesis.

3. Results

Magnetic susceptibility of $LaBi_2$ is rather anisotropic, with $\chi_{ab} > \chi_c$ (Fig. 1a). For fields applied parallel to the plane, it is constant, temperature-independent and probably dominated by Pauli paramagnetism. In-plane susceptibility rises at lower temperatures, indicating that it is dominated by low concentration of paramagnetic impurities ($<0.7\%$ assuming Gd contribution). The *c*-axis susceptibility is weakly diamagnetic and has a weak temperature dependence and a small impurity tail at low temperatures. Electrical transport of $LaBi_2$ (Fig. 1b) is metallic, linear in the temperature range above 50 K and has markedly high residual resistivity ratio ($RRR = (\rho(300\,K)/\rho(1.8\,K)) \sim 75$). Below 10 K, the resistivity curve is dominated by impurity scattering. No traces of superconductivity were observed down to 1.8 K. Analysis of $\Delta\rho$ in field (Fig. 1b inset) at 2 K reveals that it follows a linear dependence $\Delta\rho \sim H^{\alpha}$, $\alpha = 1$, close to the exponent found for $LaSb_2$, but smaller in the value of $\Delta\rho$. Fig. 2 shows specific heat of $LaBi_2$. The electronic contribution γ is very small, 2 mJ/mol K^2, and the Debye

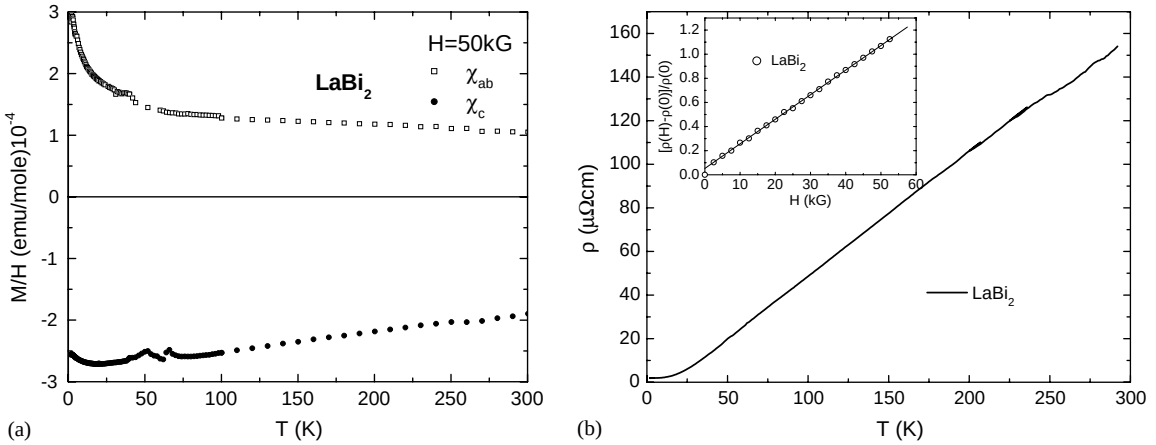

Fig. 1. (a) Magnetic susceptibility of $LaBi_2$ as a function of temperature for a magnetic field applied along the c-axis (●) and in the ab plane (□). (b) Resistivity of $LaBi_2$. Inset: Magnetoresistance at $T = 2\,K$.

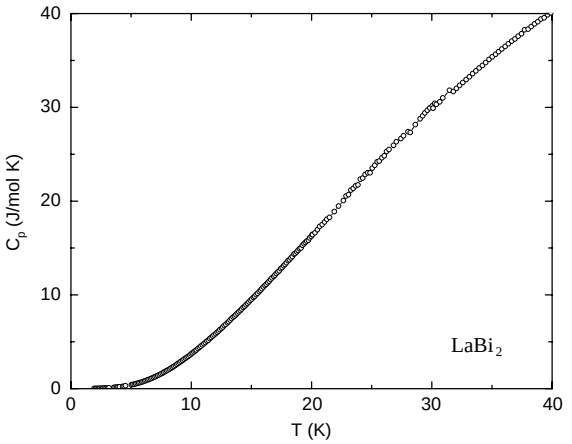

Fig. 2. Specific heat of $LaBi_2$ as a function of temperature.

temperature extracted from a fit to the specific heat data is approximately 160 K. Magnetic, thermodynamic and transport data classify $LaBi_2$ as a rather good metal with pronounced anisotropy in magnetic and possibly transport properties.

Magnetic susceptibility of $CeBi_2$ (Fig. 3a) is weakly anisotropic, with the c-axis being the hard magnetization axis. The polycrystalline average of χ^{-1} deviates from Curie–Weiss behavior (even after subtracting nonmagnetic La part) above 150 K, and fit in the range 50–150 K gives a crude estimate of the full effective magnetic moment of Ce, $\mu_{eff} = 2.83\,\mu_B$, $\theta_{poly} = -25.9$ K, $\theta_{ab} = -21.2$ K and $\theta_c = -37.1$ K. Whereas the c-axis susceptibility is indeed Curie–Weiss-like, in-plane susceptibility is distinctly non-Curie-like. The deviation of χ^{-1}_{poly} from Curie–Weiss behavior may be associated with Ce moment hybridization or incomplete $\chi(T)$ in plane data giving rise to an inaccurate estimate of χ_{poly}. Resistivity of $CeBi_2$ (Fig. 3b) has lower RRR ~ 5, and below 50 K it exhibits characteristic drop reminiscent of coherence in Kondo lattice and/or influence of depopulation of crystalline field levels. Below the temperature of magnetic ordering, a loss of spin disorder scattering is observed. Isothermal magnetoresistance curves (not shown) for various temperatures between 1.8 and 300 K displayed almost zero magnetoresistance. However, some samples have been influenced by magnetoresistance of bismuth originating from flux. A fit of specific heat data (not shown) gives an estimate of $\theta_D = 140$ K. The electronic specific heat γ is difficult to estimate from these data due to contributions from crystalline electric field split Ce moments. Magnetic isotherms (Fig. 4a) at 2 K show in-plane metamagnetism that could be associated with the rotation of spins. The magnetization does not come up to the Ce saturation moment in fields

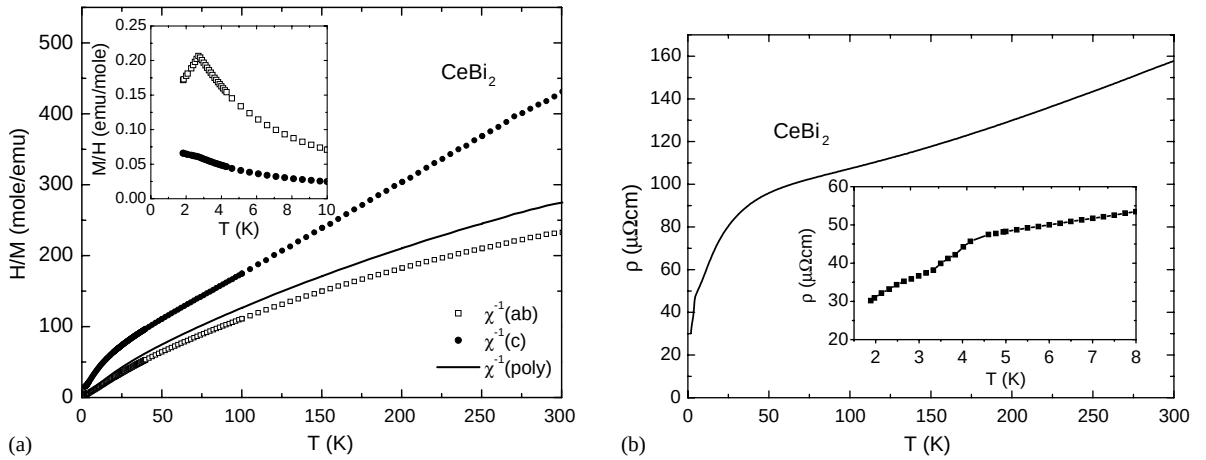

Fig. 3. (a) Inverse susceptibility of $CeBi_2$ for field applied along c-axis (●) and along basal plane (□). Solid line represents polycrystalline average. Inset: low-temperature magnetic susceptibility. (b) Resistivity of $CeBi_2$. Inset: loss of spin disorder scattering at low temperatures.

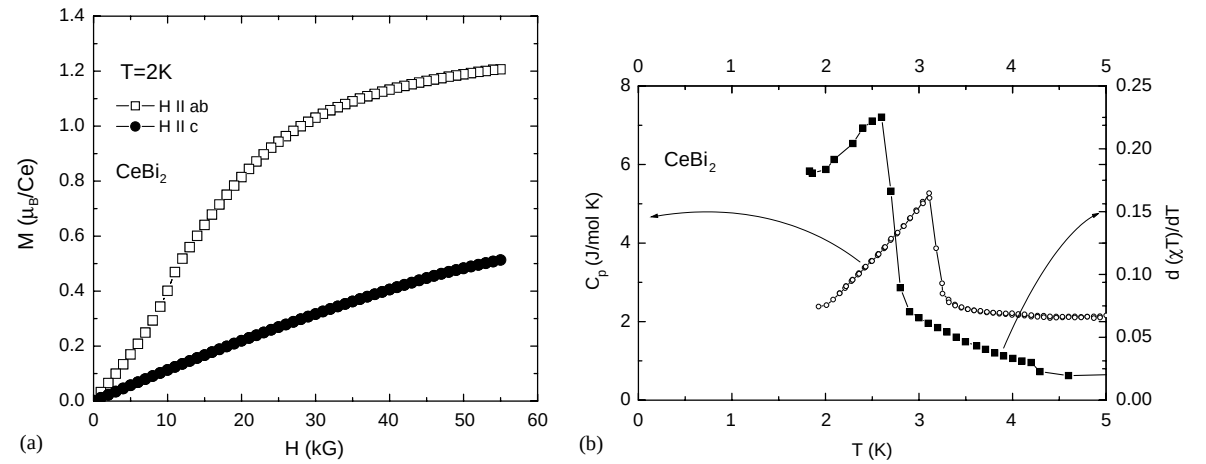

Fig. 4. (a) Magnetic isotherms of $CeBi_2$ at $T = 2\,K$ for field applied along c-axis (●) and along ab plane (□). (b) Specific heat (○) and $\partial(\chi T)/\partial T$ (■) for $CeBi_2$ at low temperatures.

up to 55 kOe, therefore, it is likely that further transitions may occur for $H > 55$ kOe. From specific heat, magnetization ($\partial(\chi T)/\partial T$) and resistivity ($\partial\rho/\partial T$), T_N values are 3.1, 2.7 and 3.75 K (Fig. 4b).

$PrBi_2$ manifests a more dramatically anisotropic magnetization (Fig. 5a) with $\chi_{ab} > \chi_c$. This difference reaches almost an order of magnitude at temperatures (~ 5 K) just above its magnetic transition. Inverse susceptibility is linear in temperature above 100 K, and polycrystalline average gives paramagnetic moment and average Curie–Weiss temperature: $\mu_{eff} = 3.52\,\mu_B$, $\theta_{poly} = -27.3$ K, whereas pronounced anisotropy is seen in $\theta_{ab} = 3.7$ K and $\theta_c = -54$ K reminiscent of anisotropy seen in $PrSb_2$.

The temperature-dependant resistivity of $PrBi_2$ (Fig. 5b) has a RRR ~ 60 and is reminiscent of $PrSb_2$, but without the high temperature anomalies that signal existence of charge or spin density wave

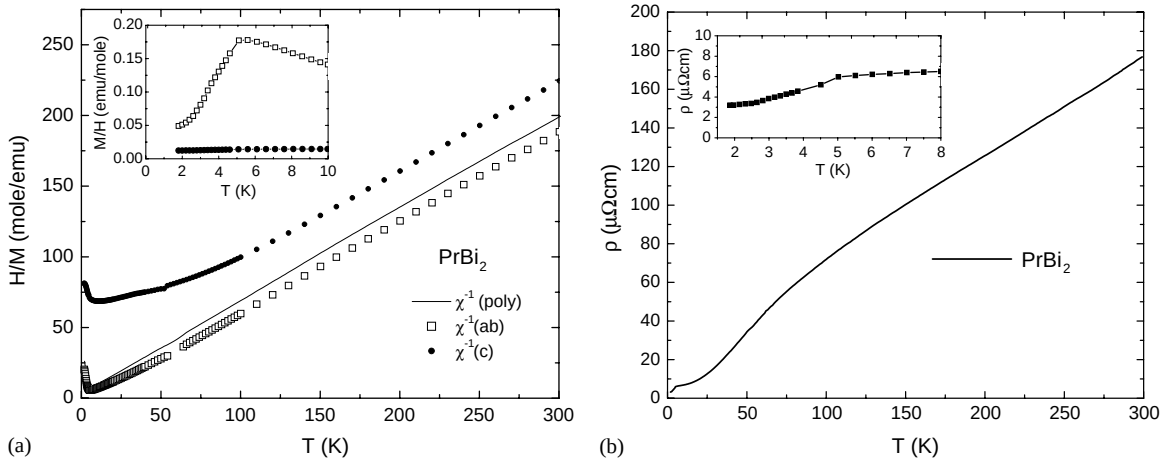

Fig. 5. (a) Inverse susceptibility of $PrBi_2$ for fields applied along c-axis (●) and ab plane (□). Solid line is polycrystalline average. Inset: anisotropy in low-temperature magnetic susceptibility of $PrBi_2$. (b) Resistivity of $PrBi_2$. Inset: low-temperature resistivity and loss of spin disorder scattering.

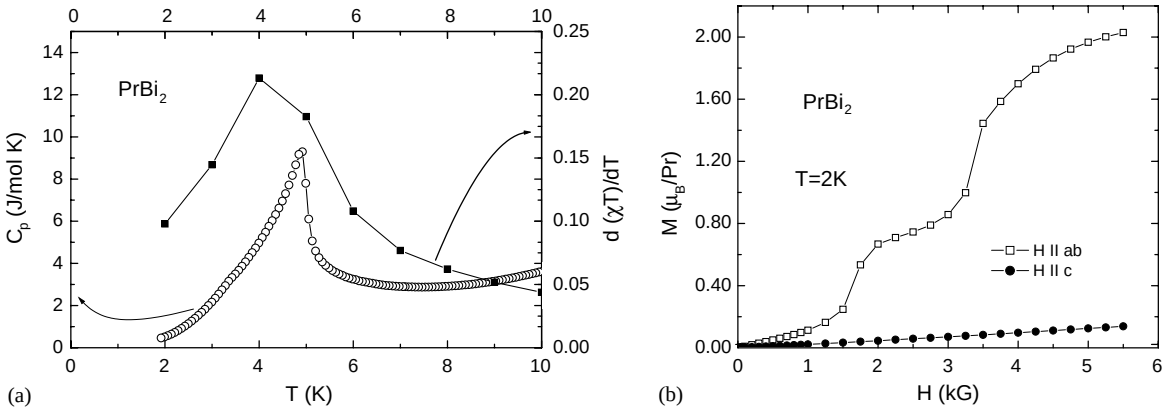

Fig. 6. (a) Specific heat (○) and $\partial(\chi T)/\partial T$ (■) of $PrBi_2$. (b) Magnetization isotherms of $PrBi_2$ at 2 K for field applied along c-axis (●) and ab plane (□).

[1]. There is a clear loss of spin disorder scattering associated with magnetic transition in the resistivity data for $PrBi_2$ at 4.5 K (Fig. 5b inset). The specific heat data on $PrBi_2$ reveals single magnetic transition below 5 K (Fig. 6a), and from its temperature dependence at higher temperature (not shown) we can estimate Debye temperature $\theta_D = 140$ K. The Neel temperature values from specific heat, magnetization and resisitivity data are 5, 4 and 4.5 K, respectively. Magnetization isotherms at 2 K (Fig. 6b) show two clear metamagnetic transitions for field applied in the ab plane, whereas for the field applied along c-axis, magnetization is linear with no signs of metamagnetism. As was the case for $CeBi_2$, $PrBi_2$ does not reach its saturation magnetization up to 55 kOe. It is therefore likely that further metamagnetic transitions may occur for $H > 55$ kOe.

$NdBi_2$ exhibits sequences of antiferromagnetic transitions probably of greater complexity than

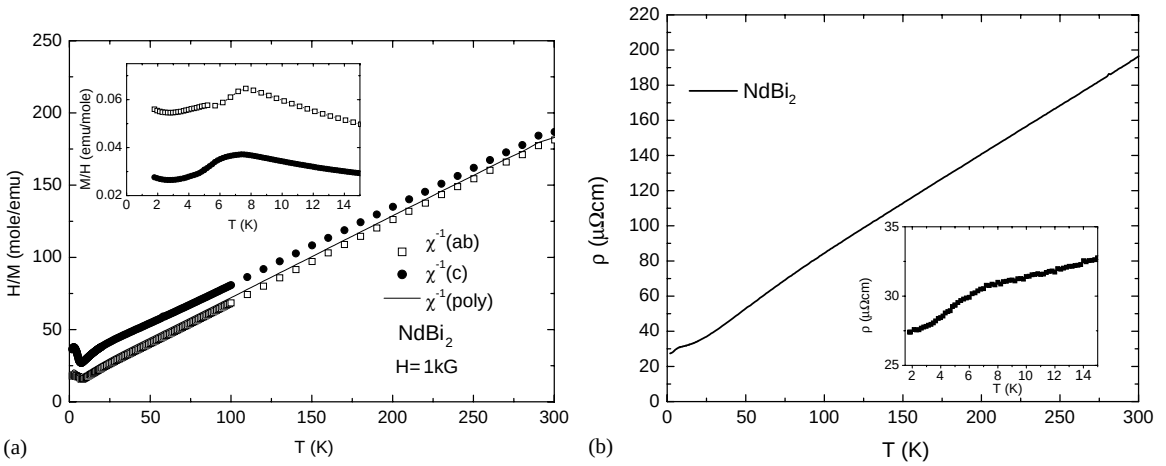

Fig. 7. (a) Inverse susceptibility of $NdBi_2$ as a function of temperature for field applied along c-axis (●) and ab plane (□). Solid line represents polycrystalline average. Inset: low-temperature magnetic susceptibility of $NdBi_2$. (b) Resistivity of $NdBi_2$. Inset: low-temperature resistivity of $NdBi_2$.

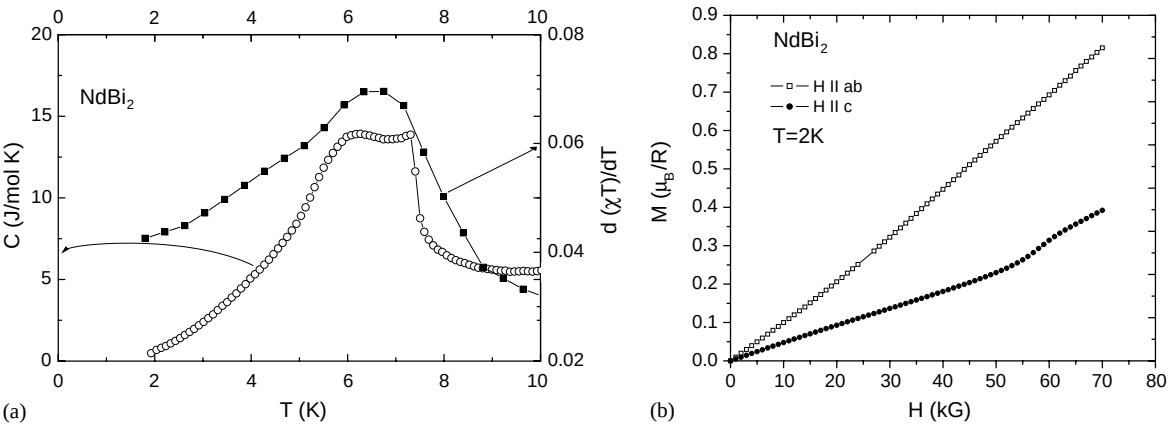

Fig. 8. (a) Specific heat (○) and $\partial(\chi T)/\partial T$ (■) of $NdBi_2$. (b) Magnetic isotherms of $NdBi_2$ at $T = 2\,K$ for fields applied along c-axis (●) and ab plane (□).

other dibismites. Upon cooling, $\chi_{ab} > \chi_c$, but anisotropy is smaller than that seen in $PrBi_2$ (Fig. 7a). Inverse susceptibility of $NdBi_2$ is Curie–Weiss-like from room temperature down to $\sim 100\,K$, consistent with effective moment of $3.77\,\mu_B$, $\theta_{poly} = -28.6\,K$, $\theta_{ab} = -19.7\,K$ and $\theta_c = -50.6\,K$. For H parallel to the ab plane, there are two clear features (maxima) in $\partial(\chi T)/\partial T$ at 7 and 4.5 K, whereas for H parallel to the c-axis, there is a broader feature at 5 K. $NdBi_2$ is metallic in the whole temperature range (Fig. 7b) with RRR ~ 7.3 and shows a broad maximum in $\partial\rho/\partial T$ at the magnetic transitions. Specific heat data (Fig. 8a) reveal rather broad magnetic transition between 7.5 and 4.8 K. The higher temperature data gave an estimate of Debye temperature $\theta_D = 140\,K$. More insight into magnetic ordered phases is seen in the magnetization data. It reveals double transition temperatures through an extremely broad maximum in $\partial(\chi T)/\partial T$, its position

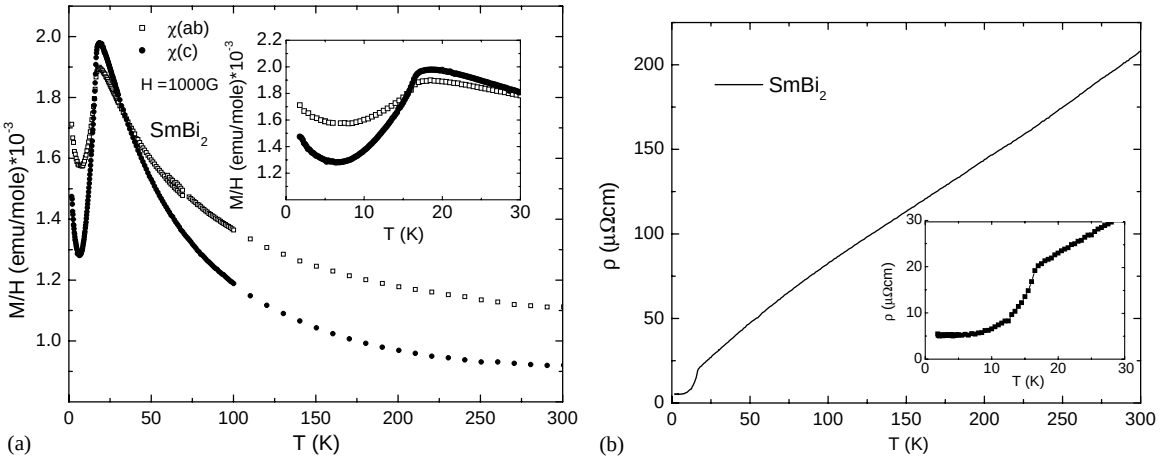

Fig. 9. (a) Magnetic susceptibility of $SmBi_2$ as a function of temperature for field applied along c-axis (●) and ab plane (□). Inset: low-temperature magnetic susceptibility. (b) Resistivity of $SmBi_2$. Inset: low-temperature resistivity.

corresponding to the specific heat. A plausible assumption could be made that magnetic ordering is accompanied with the spin reorientation process. In-plane $M(H)$ curves at 2 K (Fig. 8b) do not display any metamagnetic features until around 60 kOe, whereas no metamagnetism was seen along the c-axis in the fields up to 70 kOe. In both cases, moment values are far from the Nd^{3+} saturation value, thus more metamagnetic phases are likely to be observed at higher fields. $NdBi_2$ has negligible magnetoresistance in fields up to 70 kOe.

High-temperature susceptibility of $SmBi_2$ is not Curie–Weiss-like, probably due to the influence of Sm^{2+} ions and/or excitations out of Hunds rule ground state (Fig. 9a). Resistivity of this material (RRR ~ 40) is metallic (Fig. 9b), and there is a sharp drop associated with the loss of spin disorder scattering at the magnetic transition temperature, which is the largest found in the series, consistent with simple de Gennes scaling. The specific heat of $SmBi_2$ (Fig. 10) also reveals a single magnetic transition at 16.1 K. The Neel temperature values from specific heat, $\partial(\chi T)/\partial T$ and $\partial\rho/\partial T$ are 16.0, 16.5 and 16.0 K, respectively. An estimate of the Debye temperature gives $\theta_D = 140$ K. In addition, low-temperature magnetization data are consistent with single magnetic transition.

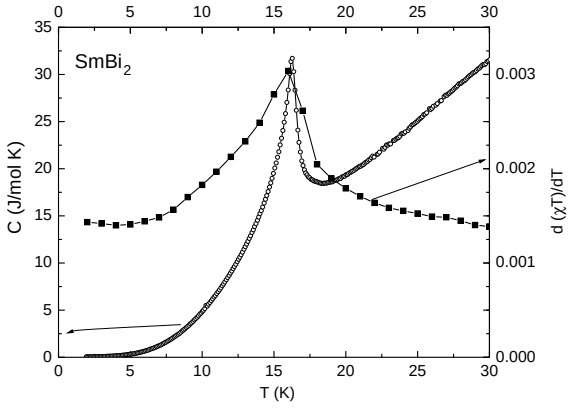

Fig. 10. Specific heat (○) and $\partial(\chi T)/\partial T$ (■) of $SmBi_2$.

4. Discussion and conclusions

The high-temperature magnetic behavior of the RBi_2 series is local moment-like and the values of the effective magnetic moment in the paramagnetic state are close to the theoretical values. All magnetic rare-earth members of the series order antiferromagnetically. The ordering temperatures, T_N, scale with the de Gennes factor $DG = [(g_J - 1)2J(J + 1)]$, where Lande g-factor is defined as $g_J = 3/2 + \{[S(S + 1) - L(L + 1)]/J(J + 1)\}$ (Fig. 11). It appears that the magnetism in metallic RBi_2

series can be described using the indirect exchange model of Rudermann–Kittel–Kasuya–Yosida (RKKY), where magnetic ordering temperature T_N is proportional to DG: $T_N \sim 8N(E_F)k_B I^2 DG$, where $N(E_F)$ is the density of states at the Fermi level, k_B is the Boltzmann constant, and I is exchange parameter. The dominant interactions along both crystalline axis for $CeBi_2$ and $NdBi_2$ are antiferromagnetic, as it can be seen in θ_c and θ_{ab} values, whereas $PrBi_2$ has a small ferromagnetic component in the ab plane. It should be noted that detailed analysis of magnetic anisotropy is possible only if in-plane anisotropy in magnetization is elucidated. Multiple transitions observed in $NdBi_2$ could be the consequence of a second-order phase transition followed by the spin reorientation process.

The magnetic entropy removed at the magnetic ordering transition for magnetic rare earths (except Pr) was obtained by subtracting specific heat of $LaBi_2$, and integrating the area under the C/T curve with respect to temperature. Due to air sensitivity, there appear to be uncertainties in specific heat measurement and estimation of magnetic entropy in this series, but Ce, Pr, and Sm are consistent with doublet and Nd is triplet or quartet of states near T_N.

Although some of the dibismites had rather low residual resistivities $\rho_0 \sim 10^{-6}\,\Omega\,\mathrm{cm}$, low-temperature magnetoresistance was not as large as in diantimonides. RRR values range from 4 to 75, roughly an order of magnitude smaller than in the case of RSb_2. Some similarity with magnetotransport of diantimonides is observed through, in specific, the near linear magnetoresistance in $LaBi_2$.

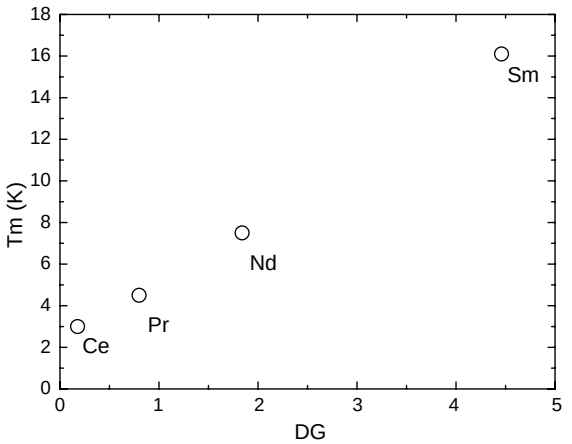

Fig. 11. De Gennes scaling of the magnetic ordering temperatures in the series.

5. Summary

We have studied the thermodynamic and transport properties of anisotropic RBi_2 series (R = La–Nd, Sm), grown as single crystals by the self-flux technique. Attempts to extend series to heavier rare earths were not successful with similar growth conditions. $LaBi_2$ is a Pauli paramagnet for fields applied along the ab plane, while it shows diamagnetic susceptibility for fields applied along the c-axis. All moment-bearing rare-earth dibismites order antiferromagnetically, with single (Ce, Pr, Sm) or double and more complex magnetic ordered phases (Nd). Sharp metamagnetism and significant metamagnetic features have been observed in $NdBi_2$ and it is possible that for this member there will be significant in-plane anisotropy. The magnetoresistance of rare-earth dibismites is close to linear with no significant anisotropy and much smaller than one observed in rare-earth diantimonides.

In general, when compared with rare-earth diantimonides, dibismites do not show the same abundance of interesting physical phenomena. However, a few points are open for further analyses: specifically, the H, T phase diagram for $PrBi_2$ and $NdBi_2$ as well as their magnetic structures in ordered state.

Acknowledgements

We thank W. Choe and G. Miller for fruitful discussions. Ames Laboratory is operated for the US Department of Energy by Iowa State University under contract No. W-7405-Eng. 892. This work was supported by the Director for Energy Research, Office of Basic Energy Sciences.

References

[1] S.L. Bud'ko, P.C. Canfield, C.H. Mielke, A.H. Lacerda, Phys. Rev. B 57 (1988) 13624.
[2] T. Kagayama, G. Oomi, S.L. Bud'ko, P.C. Canfield, Physica B 281–282 (2000) 90.
[3] A. Kagawa, T. Kagayama, G. Oomi, H. Mitamura, T. Goto, P.C. Canfield, S.L. Bud'ko, Physica B 281–282 (2000) 124.
[4] J.C.H. Mielke, N. Harrison, A.H. Lacerda, S.A. Bud'ko, P.C. Canfield, J. Phys. Condens. Matter 10 (24) (1998) 5289.
[5] K. Yoshinara, J.B. Taylor, L.D. Calvert, J.G. Despault, J. Less-Common Met. 41 (1975) 329.
[6] K. Nomura, H. Hayakawa, S. Ono, J. Less-Common Met. 52 (1977) 259.
[7] Z. Fisk, J.P. Remeika, in: K.A. Gschneider, J. Eyring (Eds.), Handbook on the Physics and Chemistry of Rare Earths, Vol. 12, Elsevier, Amsterdam, 1989.
[8] P.C. Canfield, Z. Fisk Phil. Magos. B 65 (1992) 1117.
[9] P.C. Canfield, I.R. Fisher, J. Crystal Growth 225 (2–4) (2001) 155.
[10] V.D. Abulkhaev, Izv. Ross. Akad. Nauk Met. 1 (1993) 187.